Post Hatfield rolling contact fatigue

The effect of residual stress
on contact stress driven crack growth in rail
Part 3: Further Data

A Kapoor and DI Fletcher

November 2006
NewRail Report No. WR061106-4

OFFICE OF **RAIL REGULATION**

Contents

1 Summary

This report continues from previous reports [1, 2, 3] detailing the development of crack growth models for investigating the effect of residual stress and continuously welded rail stress on running surface initiated cracks in railway rail.

This report concentrates on the prediction of crack branching direction. The use of two different residual stress distributions highlights the sensitivity of crack growth rate and direction to the residual stress distribution. Predictions are made of the branching direction for initially straight cracks at $30°$ $45°$ and $60°$ below a rail surface traversed by a driving wheel.

The findings of the modelling can be summarised as:

- Reasonably minor differences between residual stress profiles can dramatically change crack growth rate predictions. For shallow angle cracks the vertical residual stress is paramount in controlling these changes

- Residual stress promotes downward branching of shallow cracks ($30°$ below rail surface). The behaviour is independent of surface and crack face friction conditions.

- Steeper cracks ($60°$ below the rail surface) are predicted to branch in different directions at different crack lengths. Typically they are downward branching at short lengths, but longer straight cracks at the same initial angle are predicted to branch upward.

- The behaviour of cracks at $45°$ below the rail surface was found to be dependent on the residual stress distribution applied. Upward and downward branch formation is possible depending on the distribution.

- Application of CWR stress in the absence of residual stresses was predicted to produce only slight up or down branching of the cracks, with deviations of around $3°$ from the original crack path.

- Application of CWR and residual stress together was predicted to produce down-turning cracks, but with the length at which they turn down extended relative to the case with residual stress alone.

This report contains revised information on the residual stress input data, and supersedes earlier versions of the report.
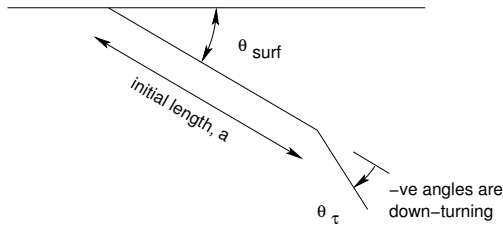
Figure 1: Definition of crack growth and branching angles
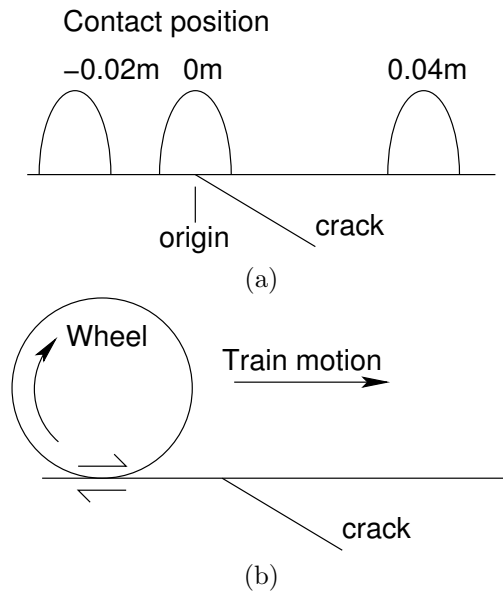
Figure 2: The rail-wheel contact. (a) Schematic illustration of contact position. (b) Simulation of a driving wheel. To provide a driving force the wheel attempts to turn marginally faster that pure rolling speed. A shear traction is produced which pushes the surface layers of the rail from right to left.

2   Introduction

2.1   Method of presenting branching data

Calculation of crack branching angles was described in the previous research report [3]. Figure 1 illustrates the sign conventions used to describe crack branching.

The branching criterion used was described in full in the project literature review [1]. Briefly, the method used was that developed by Kaneta et al. [4] based on the maximum shear stress theories (Equations 1) adapted for non-proportional loading present in rolling contact fatigue situations. The definition of the original crack angle and the branch angle are given in Figure 1. Kaneta et al. showed that the direction of branch crack growth (θ_τ) can be found by taking the root of Equation (2) relative to the initial crack growth direction which gives the maximum value of the equivalent shear mode stress intensity

4

factor K_τ . Crack growth angle and branching angles are defined by Figure 1

$$K_\tau = \frac{1}{2} \cos \frac{\theta_\tau}{2} \left[K_I \sin \theta_\tau + K_{II}(3 \cos \theta_\tau - 1) \right] \tag{1}$$

$$\tan^3 \frac{\theta_\tau}{2} - \frac{1}{\gamma} \tan^2 \frac{\theta_\tau}{2} - \frac{7}{2} \tan \frac{\theta_\tau}{2} + \frac{1}{2\gamma} = 0, \gamma = \frac{K_{II}}{K_I} \tag{2}$$

The values of K_I (tensile mode stress intensity factor) and K_{II} (shear mode stress intensity factor) at instants throughout the stress cycle (i.e. at each contact position, see Figure 2) are used to calculate crack growth direction from Equation (2) evaluated at each instant. For each contact position, the angle predicted by Equation (2) which corresponds to the maximum absolute value of stress intensity factor when substituted into Equation (1) is taken as the predicted crack growth angle.
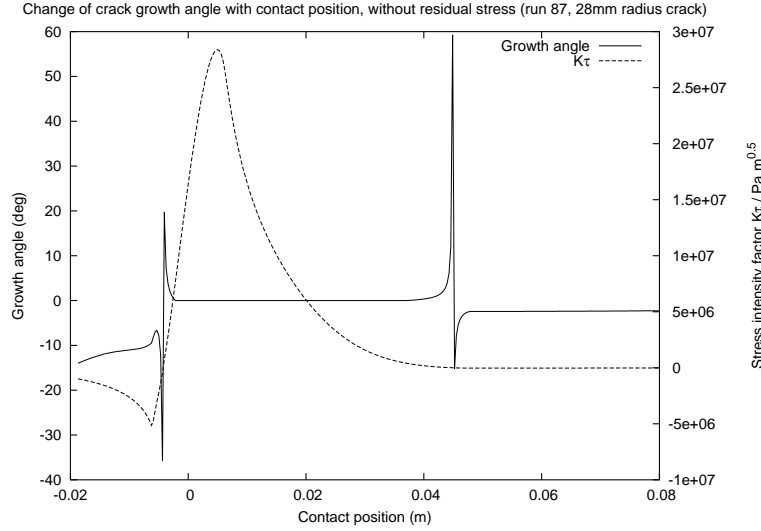
Figure 3: Example of stress intensity factor and crack growth angle variation with contact position.

Figure 3 shows a plot of these angles and the corresponding stress intensity factors for a particular contact condition and crack length, as the contact moves over the crack. From Figure 3 it can be seen that there is no single angle of growth during the passage of the contact, but that the angle varies. A reasonable assumption is that the dominant angle will correspond to the largest absolute value of stress intensity factor. An absolute value is used because in shear the sign convention simply indicates the direction of sliding, and either direction can generate cracks growth. This process must be repeated at a range of crack lengths to identify changes in growth direction as the crack extends. Figure 4(a) illustrates both positive and negative peak stress intensity factors
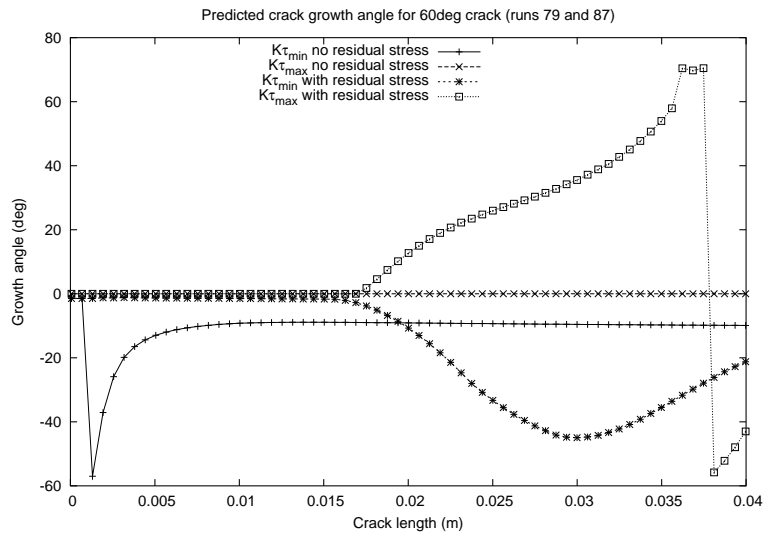
(a)
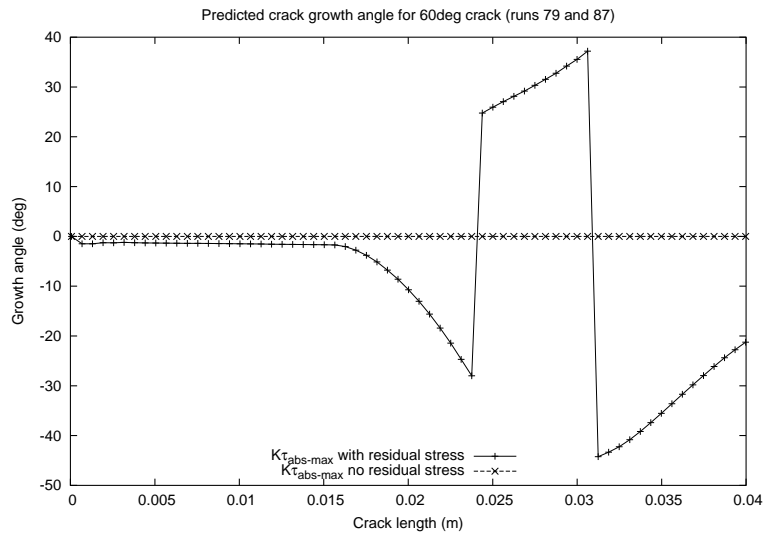
(b)

Figure 4: Example of variation of stress intensity factor and angle during the passage of a contact. (a) Positive and negative peak stress intensity factors and corresponding angles. (b) Absolute maximum stress intensity factor and corresponding angles.

6

and corresponding crack growth directions for a range of crack lengths, and Figure 4(b) shows the dominant (maximum absolute stress intensity factor) case alone. Figure 4(b) shows that at certain points in the stress cycle there is a change in the dominant peak stress intensity factor from the positive to negative peak, which leads to a change in the predicted crack growth angle. It should be remembered that the prediction shown here are for initially straight cracks, not for cracks which are progressively changing direction. A straight crack of 21mm length is predicted to turn down, while one of 25mm length is predicted to turn up. The prediction for the longer crack do not apply up a crack which turned down at a shorter length. The presence of a longer unbranched crack is possible, for example, when contact conditions change from those which favour straight crack growth, to those which favour branching - the predictions summarised by Figure 4b are for a single contact condition only.

While the identification of the peak absolute stress intensity factor provides a means to identify a dominant crack growth angle, there are cases in which the minimum and maximum peaks are similar in size, and the choice of crack growth direction may be influenced by microstructural or other features in addition to the dependence on stress intensity factor. In other cases, the peaks in stress intensity factor may differ greatly in size, and the predicted change of branch angle may be expected to take place whatever the microstructural or other features. Figure 5 illustrates the change in stress intensity factor variation with contact position which are responsible for the change in angle predicted in Figure 4b. As the crack extends, the positive peak in SIF (corresponding to the period in which the contact is directly over the crack) diminishes in width, until at 39mm crack length it disappears. Therefore, in this case, the predicted change in growth angle is the result of a substantial change in SIF, not a minor change causing the absolute maximum peak to change from the positive to negative peak.

3 Results and discussion

Because of the large number of variables investigated in the work, a single large table of runs was not useful in presenting the results. Individual tables are therefore presented for each stage of the work, followed immediately by the results and discussion. All the simulations were for cracking of the rail beneath a driving wheel (see Figure 2).

3.1 Sensitivity of crack growth rates to residual stress distribution

In the absence of residual stress data specific to the Hatfield rail previous work [2, 3] has used values from published literature [1]. To assess the sensitivity of crack growth rate to the residual stress distribution, the magnitude of these residual stresses was varied by ±25%. This showed high sensitivity of crack growth rate to changes in residual stress [3].

To further investigate the effect of different residual stress distributions on crack growth rates, a second residual stress distribution was obtained from Joe Kelleher [5]. Figure 6 shows the variation of residual stress with depth for both distributions, and Table 1 summarises the runs completed for each distribution.
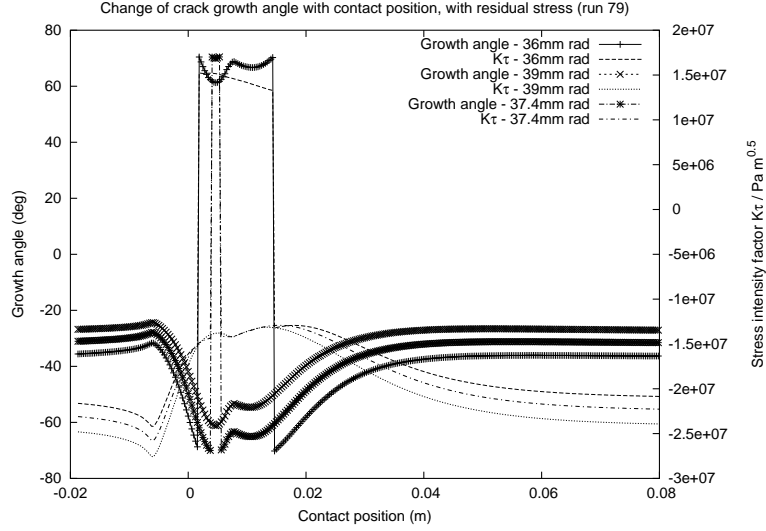
Figure 5: Example of change in stress intensity factor variation with contact position as the crack extends. Note the great difference between these plots and those shown in Figure 3.

Run no.	2d/2.5d	Residual stress	Long	Vertical
4	2d	Standard	Y	-
5	2.5d	Standard	Y	-
6	2d	Standard	-	Y
7	2.5d	Standard	-	Y
12	2d	Standard	Y	Y
13	2.5d	Standard	Y	Y
100	2d	JK	Y	Y
101	2.5d	JK	Y	Y
102	2d	JK	Y	-
103	2.5d	JK	Y	-
104	2d	JK	-	Y
105	2.5d	JK	-	Y

Table 1: Conditions examined for determining the sensitivity of crack growth rate to the residual stress distribution. All cracks at 30° below the rail surface, with surface and crack face friction coefficients of 0.18, and 1500MPa maximum Hertzian contact pressure. The "Standard" residual stress pattern is as used in the stages of the current project already reported [1, 2, 3], the modified pattern was from Joe Kelleher [5]. No residual shear stresses were included in any of the runs. Run numbers are not sequential because only those relevant to this section are presented here.
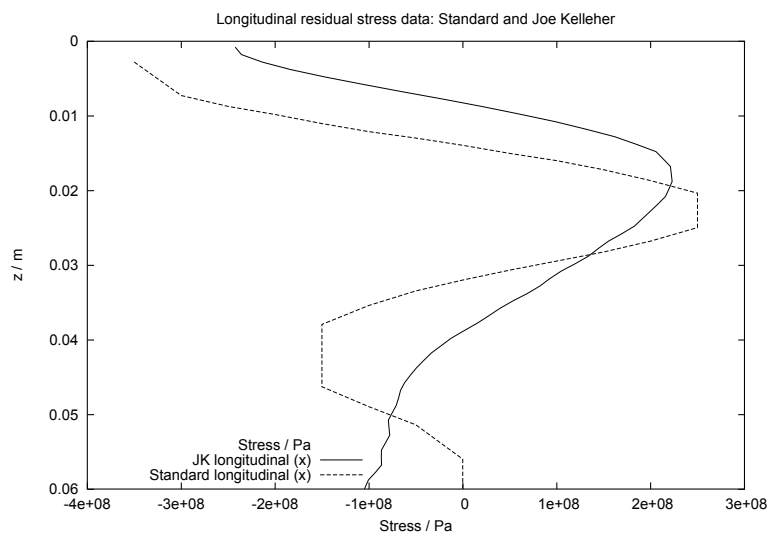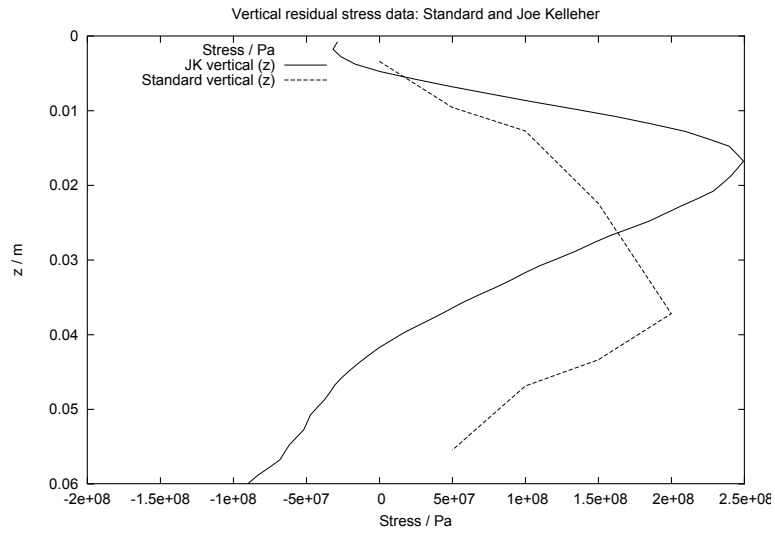
Figure 6: Comparison of residual stress distributions (below the centre of the rail head) used in the current project [2, 3], and obtained by Joe Kelleher (Manchester) [5]. (a) Vertical residual stresses. (b) Longitudinal residual stresses.

With both the longitudinal and vertical residual stresses included in the calculations, there was considerable change in growth rates for both the 2d and 2.5d contact model results with the change of residual stress input. This is illustrated in Figure 7, which shows that the JK residual stress distribution reduces crack growth rate at crack lengths below around 18mm, and very greatly accelerates growth of longer cracks.

To investigate which component of stress is responsible for the changes of crack growth shown in Figure 7, further runs were undertaken with the vertical residual stress alone (Figure 9) and with the longitudinal stress alone (Figure 8). For both the 2d and 2.5d models, the difference between the two longitudinal residual stress distributions produced only minor changes in the predicted crack growth rates, including the reductions in crack growth rate at shorter lengths. The change in vertical residual stresses was found to be responsible for the acceleration of crack growth at longer lengths in both 2d and 2.5d models. This corresponds with previous findings [3] that for shallow angle cracks the vertical residual stress is particularly important in determining crack growth rate. The two residual stress distributions appear quite similar (Figure 6), so these results indicate the sensitivity of crack growth predictions to the vertical residual stress component.
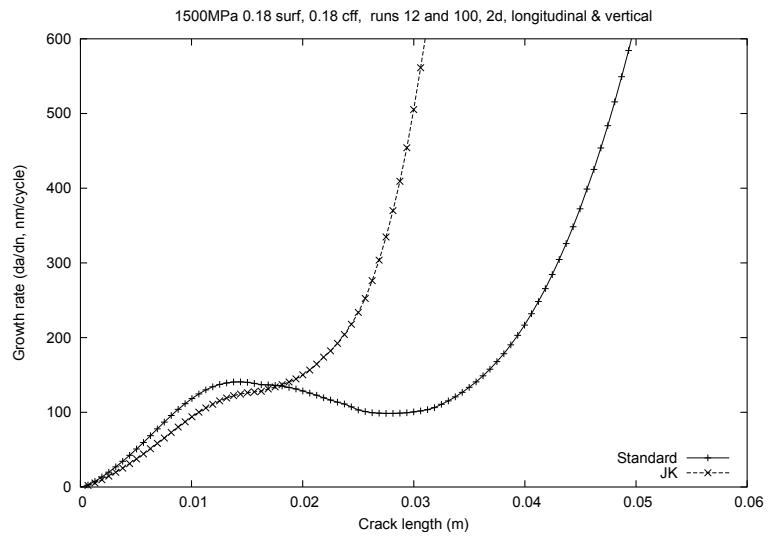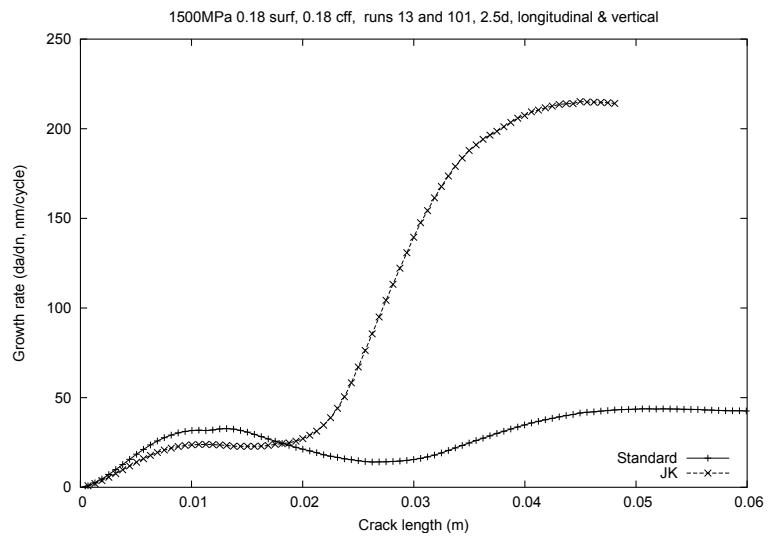
Figure 7: Comparison of crack growth rate predictions for the standard residual stress measurements used in this project [1], with those for the residual stresses predicted by Joe Kelleher (Manchester). Vertical and longitudinal residual stress included. (a) 2d model. (b) 2.5d model.
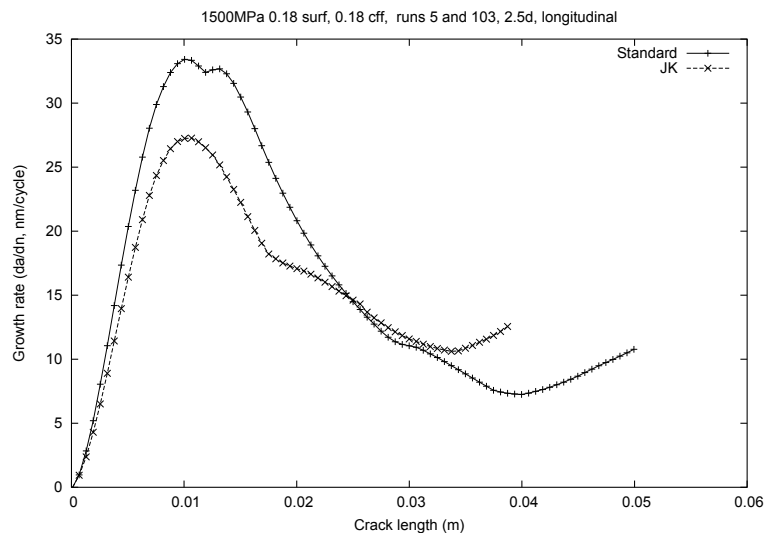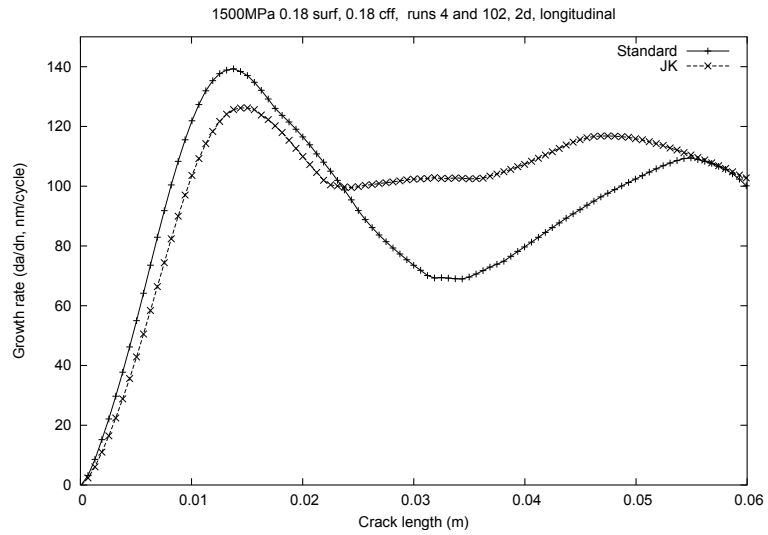
Figure 8: Comparison of crack growth rate predictions for the standard residual stress measurements used in this project [1], with those for the residual stresses predicted by Joe Kelleher (Manchester). Longitudinal residual stress only included. (a) 2d model. (b) 2.5d model.
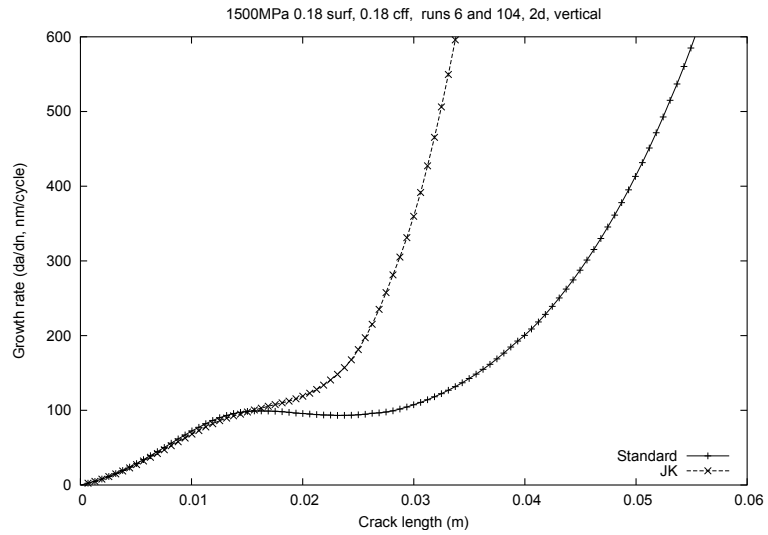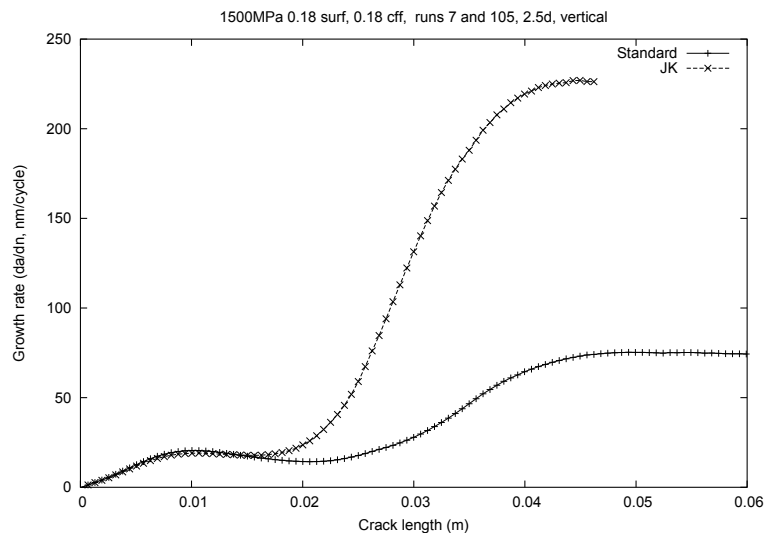
Figure 9: Comparison of crack growth rate predictions for the standard residual stress measurements used in this project [1], with those for the residual stresses predicted by Joe Kelleher (Manchester). Vertical residual stress only included. (a) 2d model. (b) 2.5d model.

13

3.2 Branching data for the standard residual stress distribution

For the standard residual stress input data used in the project [1], initial calculations have been reported previously [3] showing predictions of the effect of residual stress on crack growth rate and branching direction. Here, the work is extended to consider cracks at different initial angles and under a range of friction conditions. All the runs undertaken used the standard residual stress data, and are summarised in Table 2. Friction coefficients chosen are 0.30, 0.18 and 0.05, representing dry, water lubricated and oil lubricated contact respectively. Combinations in which crack face friction is less than surface friction coefficient are considered, representing the case of lubricant penetration of cracks followed by its removal from the rail surface (i.e. a faulty lubricator). Conditions in which crack face friction exceeds surface friction coefficient are not considered, since it is expected that lubricants will always penetrate cracks if they are present on the rail surface.

Branching results for each run are plotted in Figures 10 to 14. Rather than discussing each plot individually, it is more useful to look at the trends which emerged.

Firstly, the predictions indicate that the addition of residual stress to the contact stress cycle promotes crack branching, whereas straight crack growth was predicted in all the cases examined without residual stresses. This is significant because prediction of continuous straight crack growth does not match well with field experience, in which upward or downward branching is typical of longer cracks. Residual stresses may therefore be an important factor missing from most rail crack growth predictions until now, although factors such as rail bending will also contribute to the tendency to branch as cracks get longer.

Secondly, cracks initially at 30° or 45° below the rail surface are predicted to branch down into the rail at all crack lengths. There is a tendency to branch by around 3° when it is less than 20mm long (this which is almost completely independent of friction conditions), but at much larger angles when they exceed this length. Cracks initially at 60° below the rail surface are predicted to behave differently. They too tend to branch downward when they are short, but at 20-25mm there is a change to upward branch formation. There is a return to downward branching if a straight crack reaches 35-40mm in length. Section 2.1 explains why it is possible for the predicted branch angles of cracks to change so greatly for different crack lengths.

The results presented here are for an initially straight crack in each case because it is not currently possible to model branched cracks using the models developed and applied in this project. Because the cracks considered are straight, it may at first appear unreasonable to consider long cracks at 60° below the rail surface. However, if a shallow crack branches down (as it is predicted to do in the presence of residual stresses), its tip and the region just behind it can lie at 60° below the rail surface, as shown in Figure 15. If it is assumed that this branched crack can be approximated by an equivalent straight crack at 60° below the rail surface (shown in the figure as by Equivalent Crack 1) it is possible that a model of a crack at that angle can be used to give some guidance to likely further growth patterns and directions, although it should be borne in mind that the reliability of such an equivalent crack approach has not been verified, and that behaviour in practice will be affected by rail bending

Run no.	Residual stress	Angle deg	μ	μ_{cf}
3	-	30	0.18	0.18
15	Y	30	0.18	0.18
56	Y	30	0.30	0.30
57	Y	30	0.05	0.05
58	Y	30	0.30	0.18
59	Y	30	0.30	0.05
78	Y	45	0.18	0.18
79	Y	60	0.18	0.18
86	-	45	0.18	0.18
87	-	60	0.18	0.18
94	Y	30	0.30	0.30
95	Y	30	0.05	0.05
96	Y	30	0.30	0.18
97	Y	30	0.30	0.05
110	Y	45	0.30	0.30
111	Y	45	0.05	0.05
112	Y	45	0.30	0.18
113	Y	45	0.30	0.05
114	-	45	0.30	0.30
115	-	45	0.05	0.05
116	-	45	0.30	0.18
117	-	45	0.30	0.05
118	Y	60	0.30	0.30
119	Y	60	0.05	0.05
120	Y	60	0.30	0.18
121	Y	60	0.30	0.05
122	-	60	0.30	0.30
123	-	60	0.05	0.05
124	-	60	0.30	0.18
125	-	60	0.30	0.05

Table 2: Conditions examined for determining the effect of residual stresses on crack branching. All cracks subjected to 1500MPa maximum contact pressure, modelled using the 2.5d model. Runs included standard vertical, longitudinal and shear components of residual stress [1]. Run numbers are not sequential because only those relevant to this section are presented here.

as the crack becomes long. This and an alternative approach using Equivelent Crack 2 shown in Figure 15 are the subject of current research.

The sensitivity of these branching predictions is investigated in Section 3.4, in which the JK residual stress distribution is applied.
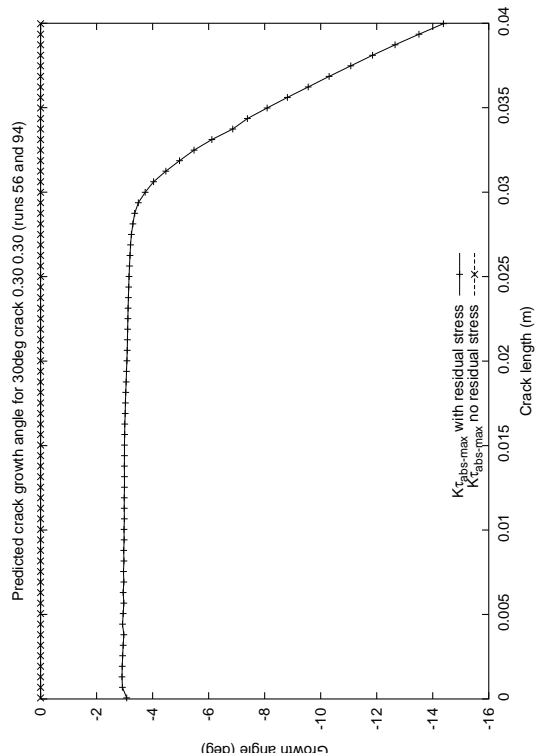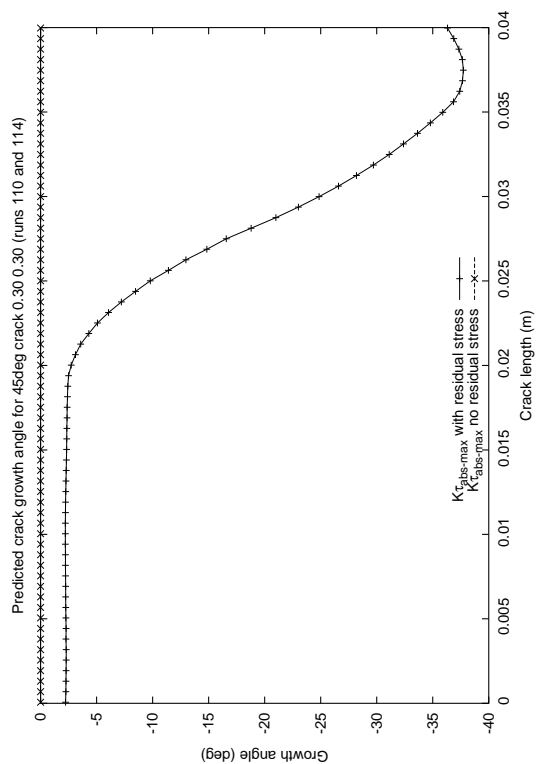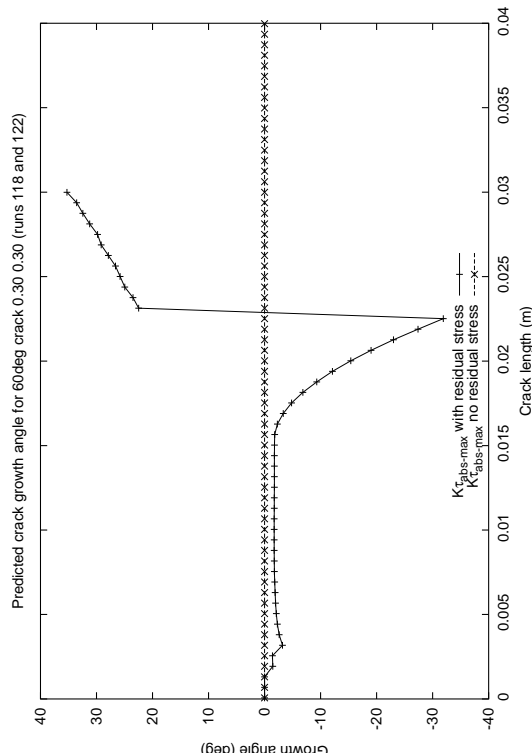
Figure 10: Crack branching direction predictions both with and without residual stress. Surface and crack face friction coefficients of 0.30. (a) 30 deg cracks. (b) 45 deg cracks. (c) 60 deg cracks. The plots for "no residual stress" lie at zero growth angle. (Runs 56/94, 110/114, 118/122)

17
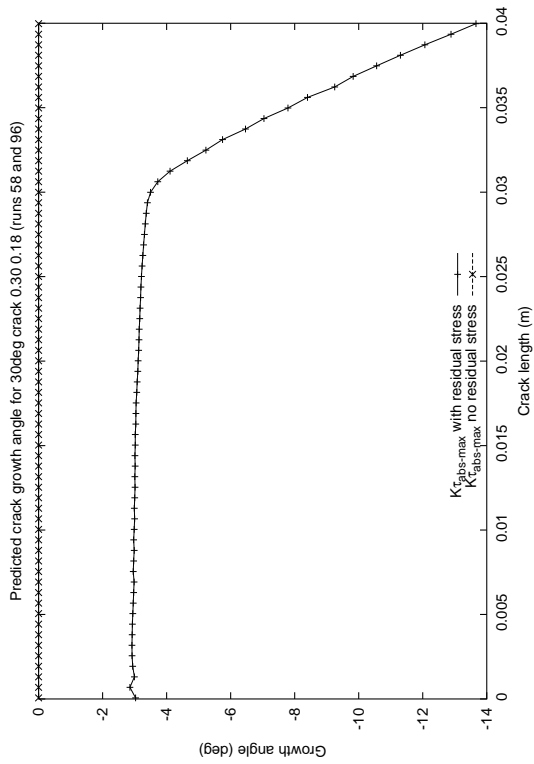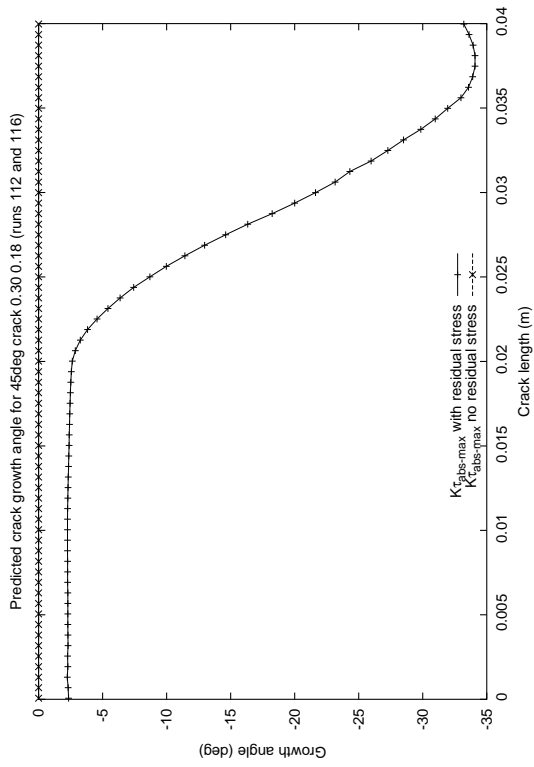
(a)

(b)
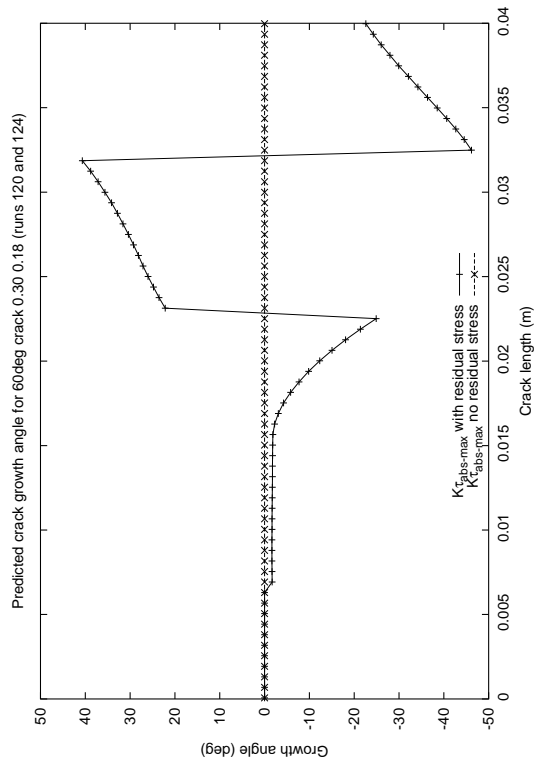
(c)

Figure 11: Crack branching direction predictions both with and without residual stress. Surface friction coefficient of 0.30 and crack face friction coefficient of 0.18. (a) 30 deg cracks. (b) 45 deg cracks. (c) 60 deg cracks. The plots for "no residual stress" lie at zero growth angle. (Runs 58/96, 112/116, 120/124)

18
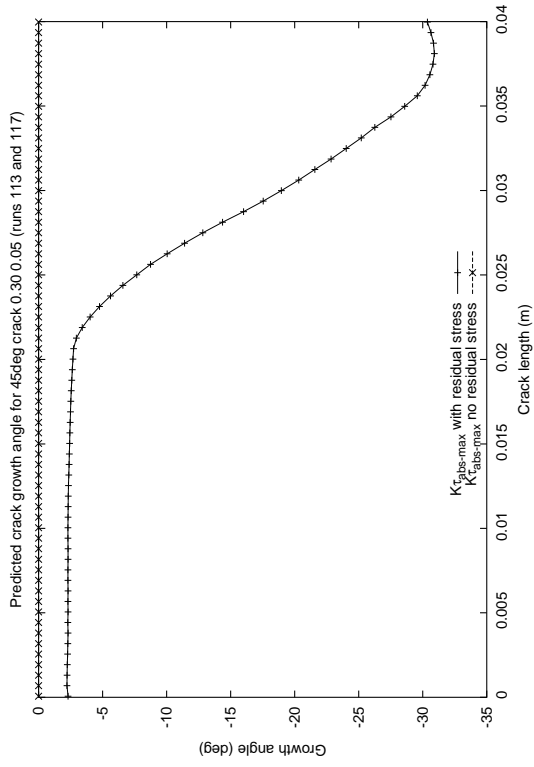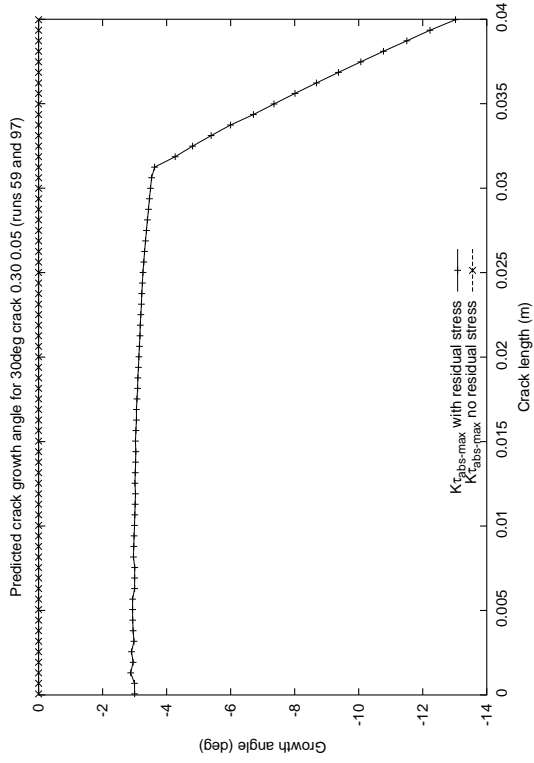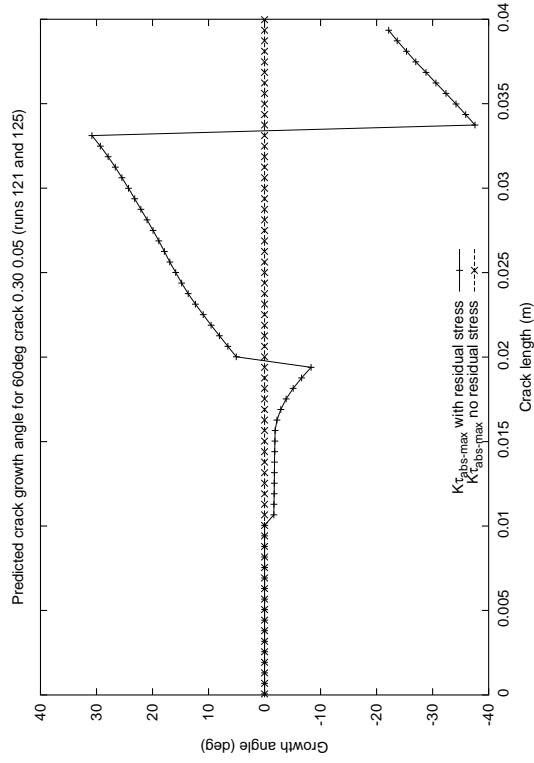
Figure 12: Crack branching direction predictions both with and without residual stress. Surface friction coefficient of 0.30 and crack face friction coefficient of 0.05. (a) 30 deg cracks. (b) 45 deg cracks. (c) 60 deg cracks. The plots for "no residual stress" lie at zero growth angle. (Runs 59/97, 113/117, 121/125)
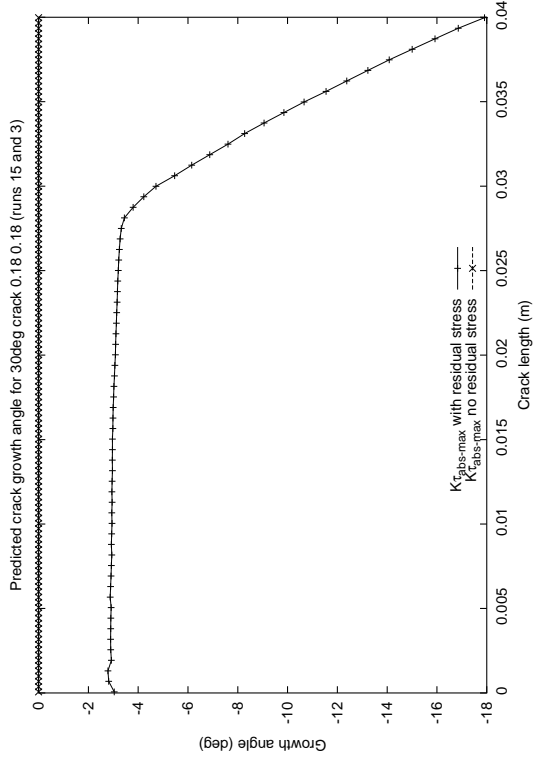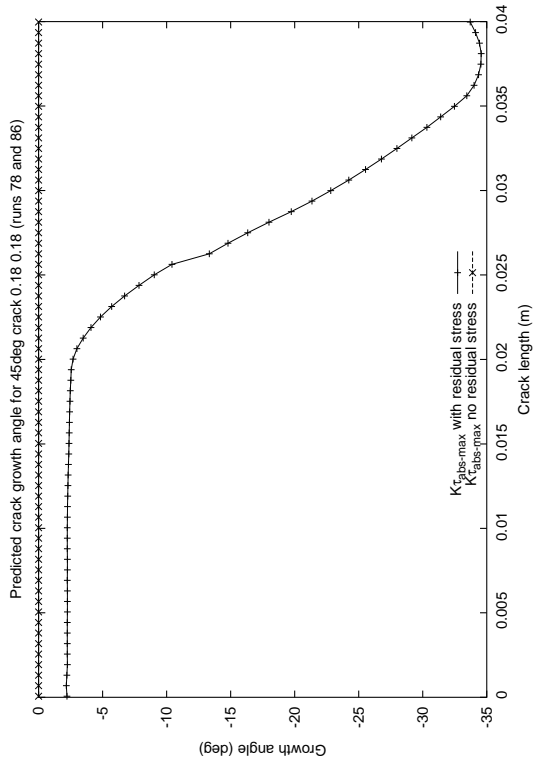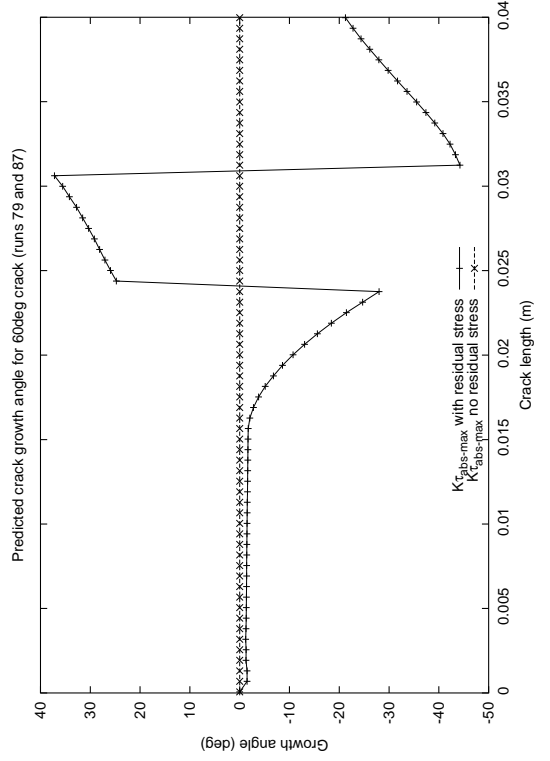
Figure 13: Crack branching direction predictions both with and without residual stress. Surface friction coefficient of 0.18 and crack face friction coefficient of 0.18. (a) 30 deg cracks. (b) 45 deg cracks. (c) 60 deg cracks. The plots for "no residual stress" lie at zero growth angle. (Runs 15/3, 15/86, 79/87)

20
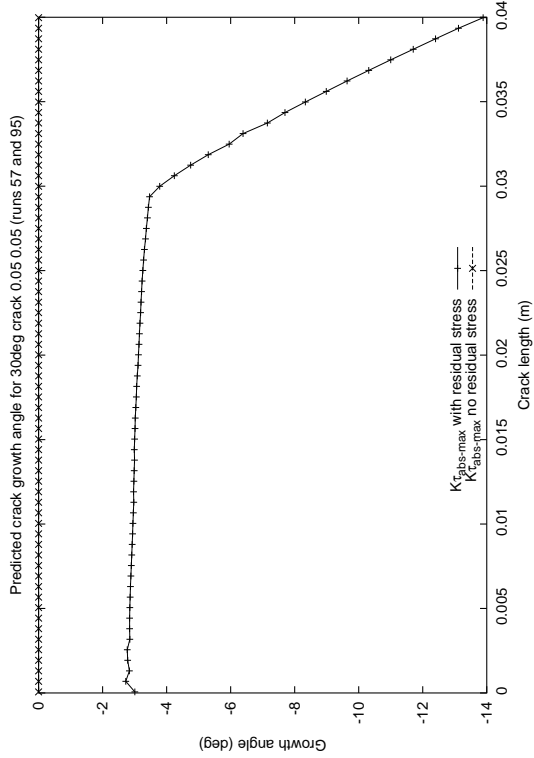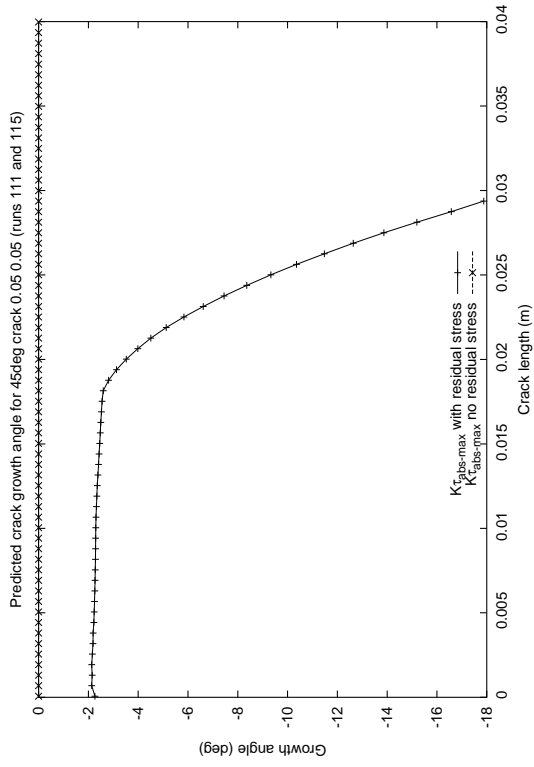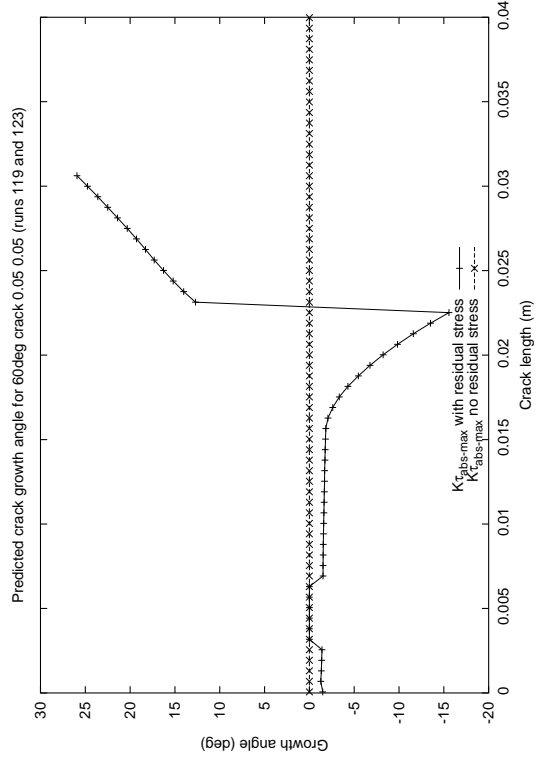
Figure 14: Crack branching direction predictions both with and without residual stress. Surface friction coefficient of 0.05 and crack face friction coefficient of 0.05. (a) 30 deg cracks. (b) 45 deg cracks. (c) 60 deg cracks. The plots for "no residual stress" lie at zero growth angle. (Runs 57/95, 111/115, 119/123)
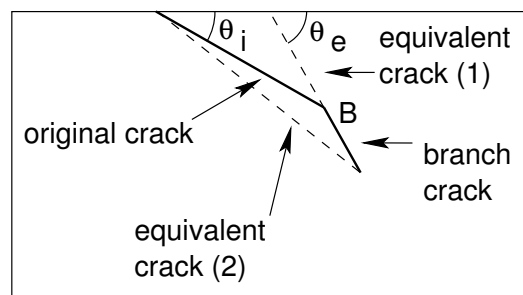
Figure 15: A crack initially at 30° below the contact surface has branched at point B. Guidance to the behaviour of the branched crack may be available by considering Equivalent Crack 1 at 60° below the surface. An alternative case considering Equivalent Crack 2 could also be investigated.

3.2.1 Crack growth rates for standard residual stress distribution

A previous report [3] presented crack growth rate results highlighting the effect of crack face friction at a constant surface traction level, and also the effect on growth rate of varying both these friction levels together. Here, results are presented for the runs detailed in Table 2, giving 5 combinations of surface traction coefficient and crack face friction coefficient for cracks at 30°, 45°, and 60° below the contact surface. Figure 16 presents the crack growth rate results.

For all the surface and crack face friction coefficient combinations examined, three trends emerge which are present in every case.

1. Without residual stress, the change of angle from 30° to 60° below the contact surface causes an increase in crack growth rate for all but the shortest crack lengths. This trend is the same as that observed previously when considering a surface and crack face friction coefficient of 0.18.

2. With residual stress applied, there is a fall in crack growth rate with increase of crack angle from 30° to 60° below the contact surface. This trend is present for all the friction conditions considered, and matches the trend identified previously at a surface and crack face friction coefficient of 0.18.

3. The ranges between growth rates predicted for cracks at 30° and those for cracks at 60° is greater for cracks with residual stress applied than for the same cracks without residual stresses present, over the majority of crack lengths considered.
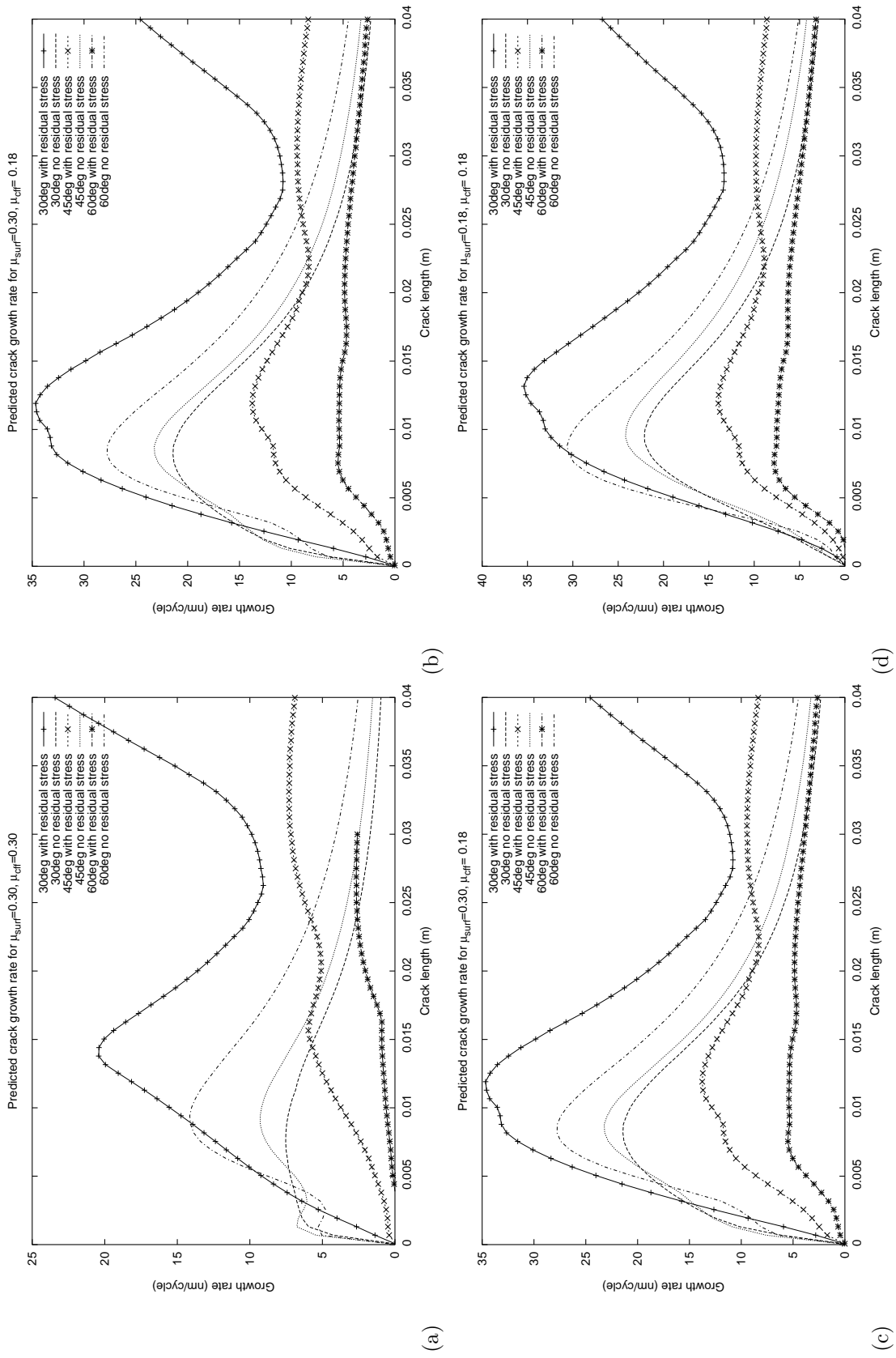
Figure 16: Crack growth rates both with and without residual stress. Surface and crack face friction coefficients: (a) both 0.30, 0.18 (c) 0.30, 0.05 (d) 0.18, 0.18 (e) 0.05, 0.05.

24
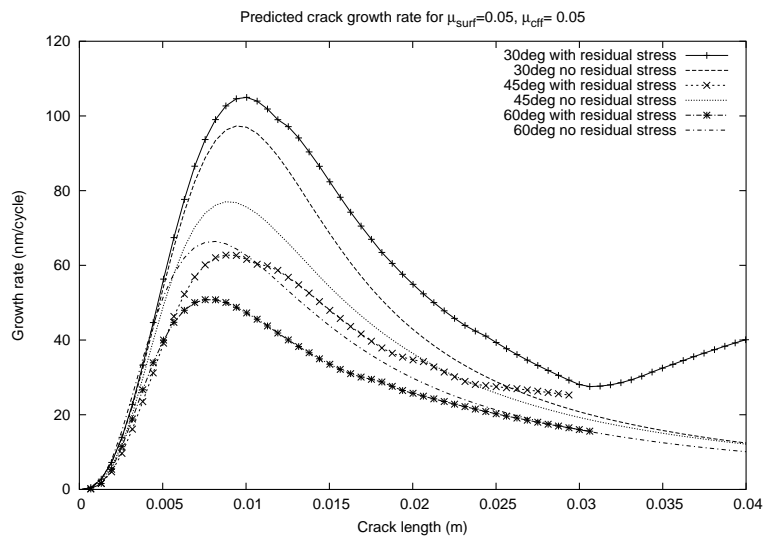
(e)

Figure 16 (continued)

3.3 Crack branching under continuously welded rail stress

The effect of continuously welded rail (CWR) stress on crack growth rate was reported in a previous report [3]. Here, the effect of CWR stress in crack branch direction is investigated using the runs summarised in Table 3. CWR stresses of ±100MPa were applied, representing a deviation of approximately $\pm40°$C relative to the rail neutral temperature.

Run no.	Residual stress	CWR MPa
3	-	-
15	Y	-
60	-	100
61	-	-100
62	Y	100
63	Y	-100

Table 3: Conditions examined for determining the sensitivity of crack branching to continuously welded rail (CWR) stress. All cracks at $30°$ below the rail surface, with surface and crack face friction coefficients of 0.18, 1500MPa maximum contact pressure, modelled using the 2.5d model. Runs included vertical, longitudinal and shear components of the standard residual stresses [1]. Run numbers are not sequential because only those relevant to this section are presented here.

Figure 17 shows the results of the CWR runs, with additional data for same contact and residual stress conditions without CWR stresses. With no residual stress applied, the application of compressive CWR stress produces a tendency for cracks initially at $30°$ below the rail surface to turn down with a branch angle of around $3°$ relative to the original crack path. This effect is crack length dependent, affecting only very short cracks, and those longer than around 20mm. Application of tensile CWR stress without residual stress causes no change in branching direction relative to that for a crack without CWR stress until lengths over 37mm, for which there is a tendency for cracks to turn slightly upward.

In the presence of residual stress, but without CWR stress, cracks initially at $30°$ below the rail surface have a tendency to turn downward, initially by around $3°$, but more steeply when the crack length exceeds 30mm (Figure 17b). The addition of CWR stresses causes no change in this pattern at short crack lengths, but delays the crack length at which cracks begin to turn more steeply down. The delay is greater for compressive CWR stress than for tensile stress.
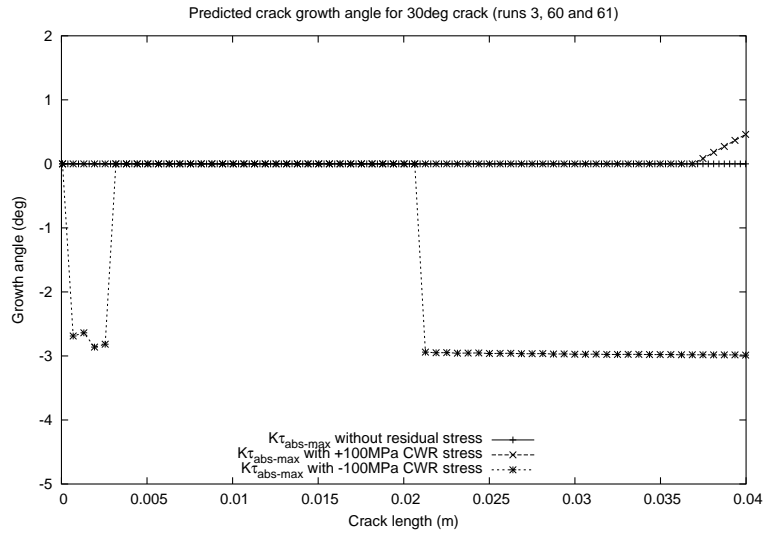
(a)
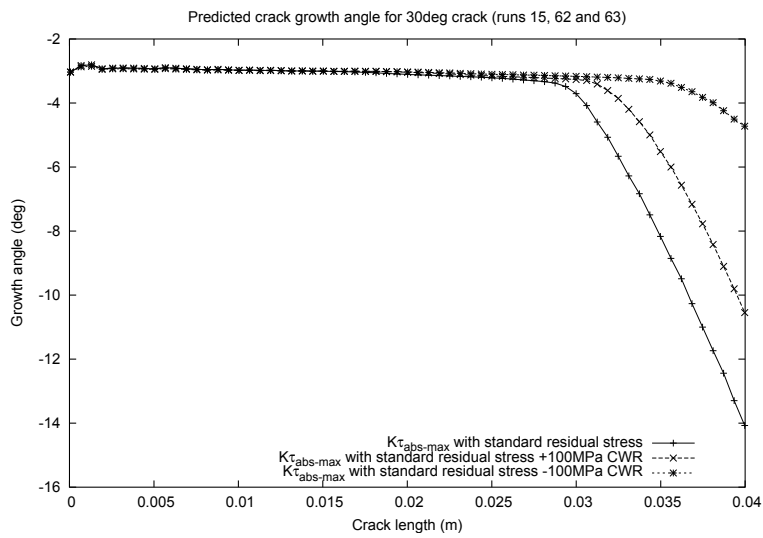
(b)

Figure 17: Crack branching direction predictions with residual stress and continuously welded rail stress (a) CWR stress alone. (b) CWR stress plus residual stress.

3.4 Crack branching data for Kelleher residual stress distribution

Section 3.2 reports crack branching results for the standard residual stress distribution used in the project [1] under a variety of contact conditions. To assess the sensitivity of crack branching to the residual stress distribution, the distribution of residual stresses from Joe Kelleher (JK) [5] was used in the runs described in Table 4. The stresses available from Joe Kelleher were from longitudinal and vertical directions only. For comparison with the standard residual stress results, addition runs with this stress distribution were also made without shear stresses present.

Run no.	Residual stress	Long	Vertical	Shear	angle 30
13	Standard	Y	Y	-	30
15	Standard	Y	Y	+Y	30
78	Standard	Y	Y	+Y	45
79	Standard	Y	Y	+Y	60
101	JK	Y	Y	-	30
106	JK	Y	Y	-	45
107	JK	Y	Y	-	60
108	Standard	Y	Y	-	45
109	Standard	Y	Y	-	60

Table 4: Conditions examined for determining the sensitivity of crack branching predictions to the residual stress distribution. All runs were at a surface and crack face friction coefficients of 0.18 with 1500MPa maximum Hertzian contact pressure, modelled using the 2.5d model. "Standard" residual stresses [1], and alternative values from Joe Kelleher [5] were used.

Figure 18 summarises the crack branching direction results for cracks at 30°, 45° and 60° below the rail surface. For the shallowest cracks, at 30°, the JK residual stress distribution produces much earlier downward branching of the cracks than for the standard residual stress distribution. Steep downward branching begins at around 21mm crack length, rather than 30mm for the standard distribution. Curves plotted for the standard distribution with and without shear stress present indicated that the removal of shear stress from the residual stresses does not have a significant effect on crack branching behaviour.

For cracks at 45° and 60° below the rail surface the picture is slightly different to the shallower cracks. In both cases, the removal of shear stress from the standard stress distribution has little effect on the predicted crack branching directions. Also in both cases, short cracks (up to around 20mm long) have a tendency to turn upwards towards the rail surface, where the standard residual stress distribution promoted slightly down-turning cracks. At longer crack lengths (greater than 20mm) there is a change to steeply downward branching cracks. For both initial crack angles, the down-turning branches at long crack lengths are steeper than are predicted for the standard residual stress distribution at similar crack lengths.
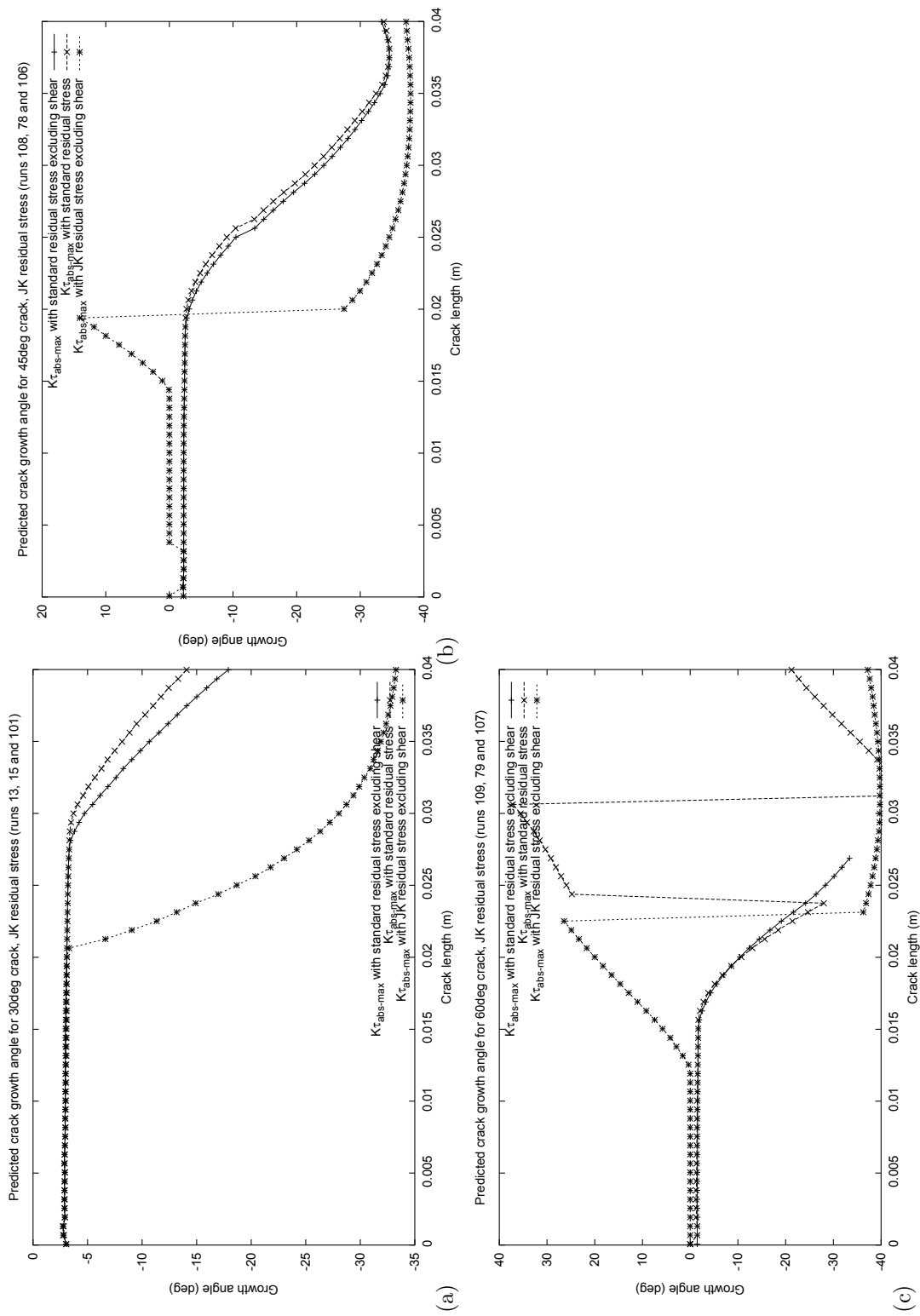
Figure 18: Sensitivity of crack branching direction to the residual stress distribution. Contact pressure 1500MPa, 2.5d model, surface and crack face friction coefficient of 0.18. (a) Crack initially at 45°. (b) Crack initially at 30°. (a) Crack initially at 60°. (Runs 13/15/101, 108/78/106, 109/79/107)

29

4   Conclusions

Results have been presented for a variety of contact conditions to investigate the effect of residual and continuously welded rail stresses on crack growth rate and branching direction. A range of residual stresses may act on a crack depending on its location in the rail head, and these stresses will also vary between rails depending on their manufacture, material properties, and loading history. Only a single set of residual stress data have been considered here, and the results are specific to those input data.

The findings of the modelling can be summarised as:

- Reasonably minor differences between residual stress profiles can dramatically change crack growth rate predictions. For shallow angle cracks the vertical residual stress is paramount in controlling these changes

- Residual stress promotes downward branching of shallow cracks (30° below rail surface). The behaviour is independent of surface and crack face friction conditions.

- Steeper cracks (60° below the rail surface) are predicted to branch in different directions at different crack lengths. Typically they are downward branching at short lengths, but longer straight cracks at the same initial angle are predicted to branch upward.

- The behaviour of cracks at 45° below the rail surface was found to be dependent on the residual stress distribution applied. Upward and downward branch formation is possible depending on the distribution.

- Application of CWR stress in the absence of residual stresses was predicted to produce only slight up or down branching of the cracks, with deviations of around 3° from the original crack path.

- Application of CWR and residual stress together was predicted to produce down-turning cracks, but with the length at which they turn down extended relative to the case with residual stress alone.

Overall, the findings indicate that crack growth rate and particularly the branching direction are highly sensitive to the specific distribution of residual stress present in the rail. It is important to remember however, that the results are for straight cracks of particular lengths, not for cracks which have branched and continued to grow. Considerable reduction of data is required to predict a single growth direction for each crack at a particular length. Where branching in two possible directions is almost equally likely, the crack may be influenced by factors such as microstructural defects, which have not been included in the current project.

References

[1] A Kapoor and D I Fletcher. Post Hatfield rolling contact fatigue. The effect of residual stress on contact stress driven crack growth in rail. Literature review. Technical Report WR061106-1, Newcastle University, November 2006.

[2] A Kapoor and D I Fletcher. Post Hatfield rolling contact fatigue. The effect of residual stress on contact stress driven crack growth in rail. Part 1: The model. Technical Report WR061106-2, Newcastle University, November 2006.

[3] A Kapoor and D I Fletcher. Post Hatfield rolling contact fatigue. The effect of residual stress on contact stress driven crack growth in rail. Part 2: Data. Technical Report WR061106-3, Newcastle University, November 2006.

[4] M Kaneta, H Yatsuzuka, and Y Murakami. Mechanism of crack growth in lubricated rolling/sliding contact. *ASLE Transactions*, 28(3):407–414, 1985.

[5] J Kelleher. Residual stress measurements processed using a contour method for an E113 rail. Private communication. 2003.